Modulation of gamma oscillations in the pedunculopontine nucleus by neuronal calcium sensor protein-1: relevance to schizophrenia and bipolar disorder

Stasia D'Onofrio, Nebojsa Kezunovic, James R. Hyde, Brennon Luster, Erick Messias, Francisco J. Urbano and Edgar Garcia-Rill

J Neurophysiol 113:709-719, 2015. First published 5 November 2014; doi:10.1152/jn.00828.2014

J Neurophysiol 113: 709–719, 2015.
First published November 5, 2014; doi:10.1152/jn.00828.2014.

Modulation of gamma oscillations in the pedunculopontine nucleus by neuronal calcium sensor protein-1: relevance to schizophrenia and bipolar disorder

Stasia D'Onofrio,[1] Nebojsa Kezunovic,[1] James R. Hyde,[1] Brennon Luster,[1] Erick Messias,[1] Francisco J. Urbano,[2]* and Edgar Garcia-Rill[1]*

[1]*Center for Translational Neuroscience, Departments of Neurobiology and Developmental Sciences and Psychiatry, University of Arkansas for Medical Sciences, Little Rock, Arkansas; and* [2]*Instituto de Fisiología, Biología Molecular y Neurociencias, Consejo Nacional de Investigaciones Científicas y Técnicas, University of Buenos Aires, Buenos Aires, Argentina*

Submitted 17 October 2014; accepted in final form 4 November 2014

D'Onofrio S, Kezunovic N, Hyde JR, Luster B, Messias E, Urbano FJ, Garcia-Rill E. Modulation of gamma oscillations in the pedunculopontine nucleus by neuronal calcium sensor protein-1: relevance to schizophrenia and bipolar disorder. *J Neurophysiol* 113: 709–719, 2015. First published November 5, 2014; doi:10.1152/jn.00828.2014.—Reduced levels of gamma-band activity are present in schizophrenia and bipolar disorder patients. In the same disorders, increased neuronal calcium sensor protein-1 (NCS-1) expression was reported in a series of postmortem studies. These disorders are also characterized by sleep dysregulation, suggesting a role for the reticular activating system (RAS). The discovery of gamma-band activity in the pedunculopontine nucleus (PPN), the cholinergic arm of the RAS, revealed that such activity was mediated by high-threshold calcium channels that are regulated by NCS-1. We hypothesized that NCS-1 normally regulates gamma-band oscillations through these calcium channels and that excessive levels of NCS-1, such as would be expected with overexpression, decrease gamma-band activity. We found that PPN neurons in rat brain slices manifested gamma-band oscillations that were increased by low levels of NCS-1 but suppressed by high levels of NCS-1. Our results suggest that NCS-1 overexpression may be responsible for the decrease in gamma-band activity present in at least some schizophrenia and bipolar disorder patients.

arousal; bipolar disorder; P/Q-type calcium channels; REM sleep; schizophrenia; waking

REDUCED GAMMA-BAND ACTIVITY was reported in bipolar disorder (Ozerdem et al. 2011). Aberrant gamma-band activity and coherence during cognitive tasks were described in schizophrenia (Ulhass and Singer 2010). Others demonstrated deficits in coherence and maintenance of gamma oscillations in patients with schizophrenia (Spencer et al. 2003). Decreases in gamma-band coherence and maintenance can account for many of the symptoms of schizophrenia. The positive symptoms include hallucinations, delusions, thought disorder, and agitation, while negative symptoms include lack of affect, anhedonia, and withdrawal. Cognitive symptoms include poor executive function, decreased attention, and disturbed working memory. Cognitive and executive functions are associated with gamma-band activity (Eckhorn et al. 1988; Gray and Singer 1989; Philips and Takeda 2009; Singer 1993). Schizophrenia is also characterized by sleep-wake symptoms such as hyperarousal, increased rapid eye movement (REM) sleep, decreased slow wave sleep, and hallucinations (Dement 1967; Garcia-Rill 2009).

Gamma-band activity also was described in the basal ganglia (Trottenberg et al. 2006), cerebellum (Lang et al. 2006), and hippocampus (Charpak et al. 1995; Chrobak and Buzsáki 1998). Coherent gamma frequencies occur between the thalamus and cortex (Pedroarena and Llinas 2001), cortex and cerebellum (Soteropoulos and Baker 2006), cerebellum and thalamus (Timofeev and Steriade 1997), and hippocampus and cortex (Buzsáki 2006). Gamma activity in the motor cortex lags behind coherent activity in subcortical structures (Lalo et al. 2008; Litvak et al. 2012), suggesting that gamma synchronization reflects an arousal-related event for enabling initiation of movement (Brucke et al. 2012; Cheyne and Ferrari 2013; Jenkinson et al. 2013). In addition, we showed that every cell in the reticular activating system (RAS), especially the pedunculopontine nucleus (PPN), plateaus at gamma frequencies (Kezunovic et al. 2011; Simon et al. 2010; Urbano et al. 2012). We made similar observations in the intralaminar thalamus (ILT), specifically the parafascicular nucleus (Pf), which relays PPN activity to the cortex (Kezunovic et al. 2012). The role of gamma activity in the PPN was proposed to underlie the process of preconscious awareness (Garcia-Rill et al. 2013): in other words, to participate in the essential mechanism that allows the uninterrupted flow of afferent sensory information necessary for the "stream of consciousness" (James 2007). We also discovered that gamma oscillations in the PPN and ILT are based on high-threshold, voltage-dependent N- and P/Q-type calcium channels (Kezunovic et al. 2011, 2012, 2013). We localized P/Q-type calcium channel-mediated oscillations to the dendrites of PPN and Pf cells (Hyde et al. 2013a,b).

In postmortem studies, increased neuronal calcium sensor protein-1 (NCS-1) expression was present in schizophrenia and bipolar disorder patients (Bergson et al. 2003; Koh et al. 2003). We tested the hypothesis that NCS-1 modulates calcium channels in PPN neurons and that excessive levels of NCS-1, as would be expected with overexpression, reduce or block gamma oscillations. Indeed, we describe a novel, concentration-dependent biphasic effect of intracellular NCS-1 on

* F J. Urbano and E. Garcia-Rill contributed equally to this work.

Address for reprint requests and other correspondence: E. Garcia-Rill, Center for Translational Neuroscience, Dept. of Neurobiology and Developmental Sciences, Univ. of Arkansas for Medical Sciences, Slot 847, 4301 West Markham St., Little Rock, AR 72205 (e-mail: GarciaRillEdgar@uams.edu).

gamma oscillations in PPN neurons. Such a mechanism would help explain the decrease in gamma-band activity seen in schizophrenia and bipolar disorder. We described preliminary data for this project in a recent poster and review (D'Onofrio et al. 2014; Garcia-Rill et al. 2014).

METHODS

Slice Preparation

Pups aged 9–13 days from adult timed-pregnant Sprague-Dawley rats (280–350 g) were anesthetized with ketamine (70 mg/kg im) until tail pinch reflex was absent. This age range was selected due to the developmental decrease in REM sleep of the rat that occurs between 10 and 30 days (Jouvet-Mounier et al. 1970). This period of investigation enabled sampling from a baseline period (9–13 days) before the epoch of the greatest transitions that peak at 14–16 days and continued until >20 days, as determined by our previous body of work on the PPN (Garcia-Rill et al. 2008). Pups were decapitated and the brain was rapidly removed and then cooled in oxygenated sucrose-artificial cerebrospinal fluid (sucrose-aCSF). The sucrose-aCSF consisted of the following (in mM): 233.7 sucrose, 26 $NaHCO_3$, 3 KCl, 8 $MgCl_2$, 0.5 $CaCl_2$, 20 glucose, 0.4 ascorbic acid, and 2 sodium pyruvate. Sagittal sections (400 μm) containing the PPN were cut, and slices were allowed to equilibrate in normal aCSF at room temperature for 1 h. The aCSF was composed of the following (in mM): 117 NaCl, 4.7 KCl, 1.2 $MgCl_2$, 2.5 $CaCl_2$, 1.2 NaH_2PO_4, 24.9 $NaHCO_3$, and 11.5 glucose. Slices were recorded at 37°C while perfused (1.5 ml/min) with oxygenated (95% O_2-5% CO_2) aCSF in an immersion chamber for patch-clamp studies as previously described (Kezunovic et al. 2011, 2012, 2013). The superfusate contained the following synaptic receptor antagonists: the selective NMDA receptor antagonist 2-amino-5-phosphonovaleric acid (APV; 40 μM), the competitive AMPA/kainate glutamate receptor antagonist 6-cyano-7-nitroquinoxaline-2,3-dione (CNQX; 10 μM), the glycine receptor antagonist strychnine (STR; 10 μM), the specific $GABA_A$ receptor antagonist gabazine (GBZ; 10 μM), and the nicotinic receptor antagonist mecamylamine (MEC; 10 μM) collectively referred to here as synaptic blockers (SB). We also used ω-agatoxin-IVA (ω-Aga; 200 nM), a specific P/Q-type calcium channel blocker, to study its effects on calcium currents. All experimental protocols were approved by the Institutional Animal Care and Use Committee of the University of Arkansas for Medical Sciences and were in agreement with the National Institutes of Health *Guidelines for the Care and Use of Laboratory Animals*.

Whole Cell Patch-Clamp Recordings

Differential interference contrast optics was used to visualize neurons using an upright microscope (Nikon FN-1; Nikon). Whole cell recordings were performed using borosilicate glass capillaries pulled on a P-97 puller (Sutter Instrument, Novato, CA) and filled with a high-K^+ intracellular solution, designed to mimic the intracellular electrolyte concentration of the following (in mM): 124 K-gluconate, 10 HEPES, 10 phosphocreatine di Tris, 0.2 EGTA, 4 Mg_2ATP, and 0.3 Na_2GTP; or a high-Cs^+/QX-314 intracellular solution containing the following (in mM): 120 $CsMeSO_3$, 40 HEPES, 1 EGTA, 10 TEA-Cl, 4 Mg-ATP, 0.4 mM GTP, 10 phosphocreatine, and 2 $MgCl_2$. NCS-1 (Prospec, Ness-Ziona, Israel) was dissolved in the intracellular solution needed to perform each set of experiments at the concentrations described in RESULTS. All recording electrodes had 1.2 μl of standard intracellular solution injected at the tip, and the remainder of the pipette was filled with the solution (18–20 μl) of the concentration of NCS-1 to be tested. This allowed control recordings to be obtained soon after patching, while also allowing NCS-1 to diffuse into the cell. The large volume in the pipette ensured that the concentration to which the cell was exposed was stable throughout the recording period. In initial experiments, we attempted to tip load the NCS-1 but could not obtain reliable gigaseals. Therefore, having the tip filled with regular intracellular solution allowed good seal formation and a reservoir of stable concentration of NCS-1 to diffuse into the cell. Osmolarity was adjusted to ~270–290 mosM and pH to 7.3. The pipette resistance was 2–5 MΩ. All recordings were made using a Multiclamp 700B amplifier (Molecular Devices, Sunnyvale, CA) in both current- and voltage-clamp mode. Digital signals were low-pass filtered at 2 kHz and digitized at 5 kHz using a Digidata-1440A interface and pClamp10 software (Molecular Devices).

We tested the hypothesis that low levels of NCS-1 would promote neuronal activity, specifically beta/gamma-band oscillations, mediated by high-threshold, voltage-dependent calcium channels during current-clamp ramp-induced depolarization. Based on our previous findings, PPN neurons could not be depolarized beyond −25 mV using square steps due to the activation of potassium channels during rapid depolarization, instead requiring ramps to reach highly depolarized levels (Kezunovic et al. 2011, 2013). These findings revealed one of the main characteristics of PPN neuronal gamma-frequency oscillations, showing that the membrane potential at the soma had to be gradually depolarized up to approximately −20 mV (using 2-s current ramps) to activate high-threshold, voltage-dependent P/Q-type calcium channels, and to a lesser extent, N-type calcium channels, that mediate high-frequency oscillations. That is, we found that P/Q-type channels were essential for eliciting the oscillations, but N-type channels were only permissive (Kezunovic et al. 2011). The membrane potential at the dendrites, where these calcium channels are located (Hyde et al. 2013a,b), was closer to physiological levels. Thus we chose to use 1-s-long depolarizing current ramps to gradually change membrane potential from resting values up to 0 mV in current-clamp mode. This protocol applied a 700-pA, 1-s duration current ramp, executed shortly after first breaking into the cell and every 5 min thereafter, for up to 30 min. This allowed us to determine the effects of NCS-1 on PPN membrane oscillatory activity while the NCS-1 diffused into the cell.

The neurons were localized in the pars compacta in the posterior PPN, which is easily identified in sagittal sections of the brainstem (Kezunovic et al. 2011; Simon et al. 2010). The recording region was located mainly in the pars compacta in the posterior PPN, immediately dorsal to the superior cerebellar peduncle. This area of PPN has been shown to have the highest density of cells (Wang and Morales 2009; Ye et al. 2010). Gigaseal formation and further access to the intracellular neuronal compartment were achieved in a voltage-clamp configuration mode, setting the holding potential at −50 mV (i.e., near the average resting membrane potential of PPN neurons). Within a short time after rupturing the membrane, the intracellular solution reached equilibrium with the pipette solution without significant changes in either series resistance (ranging 5–12 MΩ) or membrane capacitance values. We first identified PPN neurons by cell type as previously described (Garcia-Rill et al. 2007, 2008; Simon et al. 2010). PPN cell type I PPN neurons (LTS current), type II PPN cells (Ia current), and type III PPN neurons (LTS + Ia currents) were identified as previously described (Kezunovic et al. 2011, 2012, 2013). For eliciting oscillations, the membrane potential was depolarized using a 1-s duration ramp current-clamp protocol. Voltage-dependent calcium currents (I_{Ca}) were studied using a high-Cs^+/QX314 pipette solution (in mM: 120 $CsMeSO_3$, 40 HEPES, 1 EGTA, 10 TEA-Cl, 4 Mg-ATP, 0.4 mm GTP, 10 phosphocreatine, and $MgCl_2$). Cesium and TEA-Cl are widely used potassium channel blockers. Calcium currents were recorded in the presence of extracellular synaptic receptor antagonists (Kezunovic et al. 2011, 2012, 2013) and the sodium and potassium channel blockers tetrodotoxin (TTX; 3 μM) and TEA-Cl (25 μM), respectively. Square voltage steps were used to generate PPN neuronal calcium currents from a holding potential of −50 mV and then depolarized up to 0 mV. Both series resistance and liquid junction potential were compensated (>14-kHz correction bandwidth; equivalent to <10-ms lag). Average

bridge values in current clamp were 12 ± 2 MΩ (n = 42, with 12 control cells and 25 tested with NCS-1, and 5 tested using ω-Aga). We also recorded another 27 cells in the voltage-clamp studies on calcium currents. Table 1 provides a listing of the number of animals used and number of cells recorded for each of the properties tested. No significant rundown due to intracellular dialysis of PPN neuron supra- or subthreshold activity was observed during our recording period for control PPN neurons (up to 60 min).

Drug Application

Bath-applied drugs such as SB were administered to the slice via a peristaltic pump (Cole-Parmer, Vernon Hills, IL) and a three-way valve system such that solutions reached the slice 1.5 min after the start of application. The sodium channel blocker TTX was purchased from Sigma-Aldrich (St. Louis, MO). Channel blockers were purchased from either Peptide International (Louisville, KY) or Alomone Laboratories (Jerusalem, Israel). Cholinergic antagonists were purchased from Sigma Aldrich [mecamylamine (MEC; 10 μM), a nicotinic receptor antagonist, and tetraethylammonium (TEA) a wide-range K^+ channel blocker]. NCS-1 (human recombinant) was purchased from Prospec Protein Specialist (Ness-Ziona, Israel). The effects of NCS-1 on single cell oscillatory activity were studied by allowing passive diffusion of NCS-1 (with 1.2 μl of standard intracellular solution first loaded into the pipette tip, followed by 18–20 μl of the concentration of NCS-1 to be tested) intracellularly through the recording micropipette, during extracellular superfusion of SB, channel blockers, and TTX in aCSF extracellular solution.

Data Analysis

Off-line analyses were performed using Clampfit software (Molecular Devices, Sunnyvale, CA). As stated above, we used 1-s duration ramps applied every 5 min in current lamp in the presence of SB and TTX to record membrane oscillations in all three PPN cell types. Peak oscillatory amplitude was analyzed by first filtering each ramp recording and measuring the three highest amplitude oscillations to derive a mean amplitude induced during each ramp. The mean peak frequency of the same three oscillations was filtered (high pass 10 Hz, low pass 120 Hz) and measured to derive a mean frequency of oscillations during the three highest amplitude oscillations in each ramp. The power of each frequency was also analyzed by composing a power spectrum for the frequencies in the entire ramp, giving a measure of peak power for frequency. Comparisons between groups were carried out using one-way ANOVA, with Bonferroni post hoc testing for multiple comparisons. For comparisons of effects of each concentration of NCS-1 over time, we used repeated-measures ANOVA with Bonferroni post hoc testing using SAS Proc Mixed software (SAS Institute, Cary, NC). Power spectra were composed for both voltage-clamp and current-clamp recordings using unfiltered and filtered 1-s ramps. F values and degrees of freedom are reported for all linear regression ANOVAs. Differences were considered significant at values of $P \leq 0.05$. All results are presented as means ± SE.

Table 1. *PPN cells tested with NCS-1*

Property	No. of Pups	No. of Cells
Control	5	12
NCS-1 (0.5 μM)	5	7
NCS-1 (1 μM)	3	5
NCS-1 (5 μM)	5	9
NCS-1 (10 μM)	3	4
NCS-1 (1 μM + Aga)	4	5
I_{Ca} NCS-1 (0.5 μM)	6	13
I_{Ca} NCS-1 (1 μM)	5	9
I_{Ca} NCS-1 (10 μM)	3	5
Total	39	69

PPN, pedunculopontine nucleus; NCS-1, neuronal calcium sensor protein-1; Aga, agatoxin. I_{Ca}, voltage-dependent calcium currents.

RESULTS

Whole cell patch-clamp recordings were performed in a total of 69 PPN neurons and their responses to depolarizing 1-s current ramps, in the presence of NCS-1 and SB + TTX, were used to determine the voltage dependence of their oscillatory behavior as previously described (Kezunovic et al. 2011, 2013). No difference in average resting membrane potential was observed among PPN neuronal types. A group of control neurons (n = 12) were patched using normal intracellular recording solution and tested using 1-s ramps applied shortly after patching and then in 5-min intervals for up to 30 min. The average amplitude (2.2 ± 0.5 mV) and frequency (43 ± 2 Hz) of the oscillations were similar to those observed in previous studies in the absence of stimulation with carbachol or modafinil (Kezunovic et al. 2011, 2013). As previously observed, beta/gamma oscillations were present without rundown of high-threshold, voltage-dependent calcium channel mediated responses. Using repeated-measures ANOVA, we determined that the amplitude and frequency of the ramp-induced oscillations at *minute 0* (zero) were not statistically different from those of the subsequent ramps at 5 min through 30 min (df = 6, F = 2.12, P = NS for amplitude; df = 6, F = 1.22, P = NS for frequency) in control cells. We then tested the amplitude and frequency of ramp-induced oscillations at *minute 0* in the control cells against each of the subsequent groups of cells in which NCS-1 was present in the pipette at *minute 0*. The amplitude and frequency of oscillations were not statistically different between *minute 0* in control cells and each *minute 0* recording with NCS-1 at any concentration (df = 4, F = 2.42, P = NS for amplitude; df = 4, F = 2.16, P = NS for frequency). Therefore, we concluded that the *minute 0* recordings with intracellular NCS-1 were indeed similar to control recordings.

We then studied the effects of different concentrations of NCS-1 using depolarizing ramps to induce membrane oscillations in all three groups of cells present at the PPN. Ramps were induced immediately after patching while the NCS-1 diffused passively into the neuron. Initial experiments were performed to determine the effects of NCS-1 at low concentration (1 μM) compared with very high concentration (10 μM) within the recording pipette for their effects on ramp-induced gamma frequency oscillations. We then developed a dose-response curve for NCS-1 concentrations of 0.5, 1, 5, and 10 μM. This was followed by the study of calcium currents in another group of PPN neurons to determine the effects of NCS-1 at 0.5, 1, and 10 μM on these currents, and NCS-1 at 1 μM with ω-Aga (see Table 1 for cell numbers).

Effects of 1 μM NCS-1 on Gamma-Band Oscillations in PPN Neurons

During recordings in PPN neurons, in the presence of SB + TTX, 1 μM NCS-1 increased the amplitude and frequency of ramp-induced oscillations within ~25 min of diffusion into the cell. Figure 1 is a representative example of ramp-induced membrane potential oscillations in a single PPN neuron in the presence of SB + TTX. Shortly after patching, the ramp

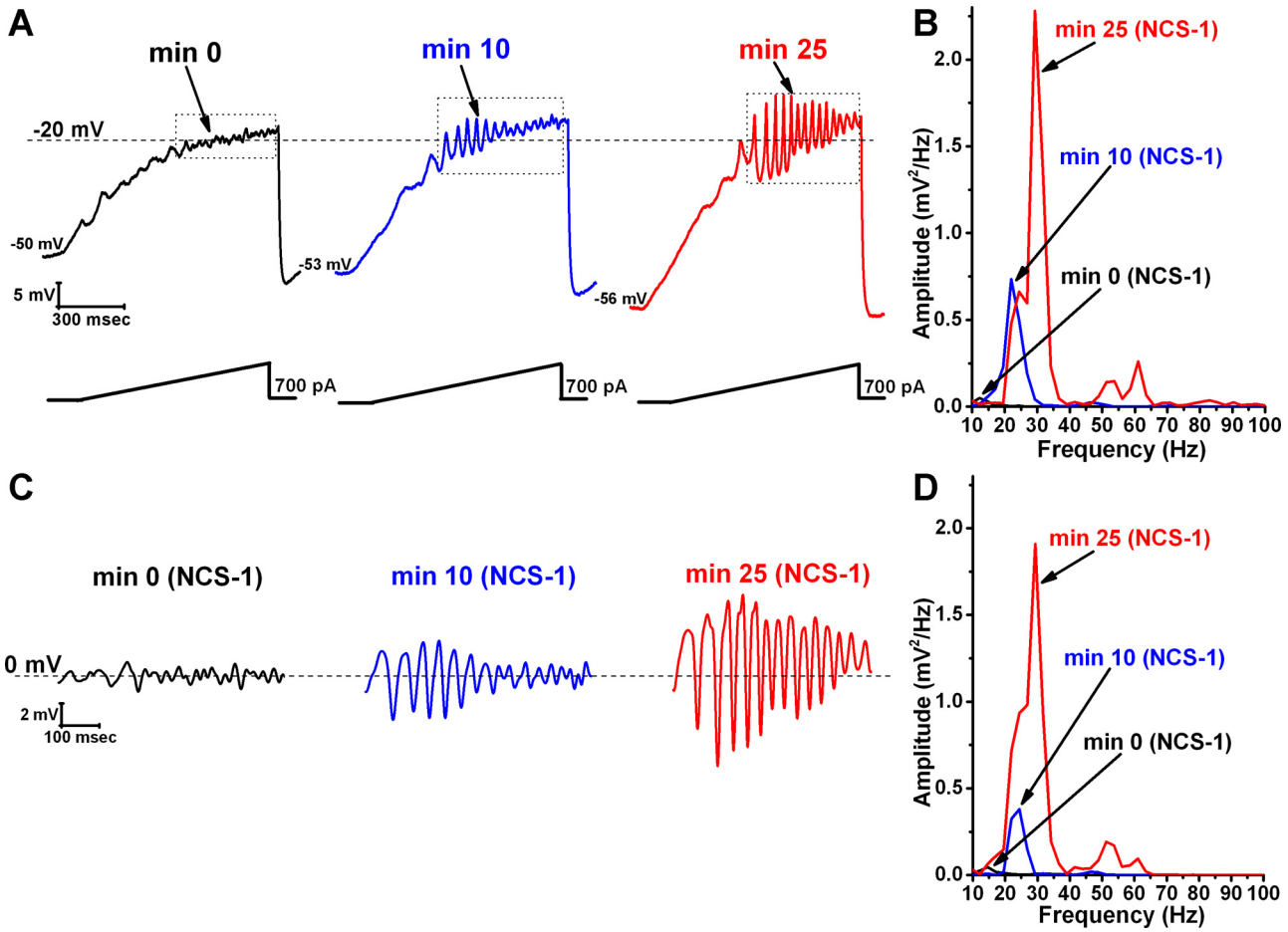

Fig. 1. Effects of neuronal calcium sensor protein-1 (NCS-1) at 1 μM on ramp-induced oscillations in pedunculopontine nucleus (PPN) neurons. *A*: representative 1-s long current ramp-induced oscillations in a PPN neuron in synaptic blockers (SB) + tetrodotoxin (TTX) extracellular solution and 1 μM NCS-1 in the recording pipette (*left*, black record). After 10 min of NCS-1 diffusing into the cell, the oscillatory activity increased slightly (*middle*, blue record). However, after 25 min of NCS-1 diffusion both oscillation amplitude and frequency were increased (*right*, red record). *B*: power spectrum of the records shown in *A* before band-pass filtering, showing the increased amplitude and frequency of oscillations after 25-min exposure to 1 μM NCS-1. *C*: records enclosed by the dotted boxes shown in *A* after band-pass filtering (high pass 10 Hz, low pass 120 Hz). *D*: power spectrum of the records shown in *C* after band-pass filtering. Dashed lines in *A* represent the −20-mV membrane potential and dashed lines in *C* represent the 0-mV membrane potential. The small decrease in power may be due to the use of filtering.

typically induced low amplitude oscillations in the beta/gamma range (black record in Fig. 1*A* and in Fig. 1*B* as a black line in the power spectrum). Figure 1*A*, blue record, shows that, after 10 min of recording, some increase in the oscillation frequency was present (also evident in Fig. 1*B* as a blue line in the power spectrum). After 25 min of recording, NCS-1 at 1 μM significantly increased the frequency of oscillations (red record in Fig. 1*A* and as the red line in the power spectrum). We then filtered the ramp in each record using 10-Hz low pass and 120-Hz high pass to eliminate low frequencies. Figure 1*C* shows the band-pass-filtered recordings of the ramps shown in Fig. 1*A* with NCS-1 at 1 μM immediately upon patching (black record, 0 min), 10 min after patching when some NCS-1 had diffused into the cell (blue record), and after 25 min of patching when oscillations had reached their maximal amplitude (red record). Figure 1*D* is a power spectrum of the filtered records in Fig. 1*C*. The spectrum showed a clear enhancement in both the frequency and amplitude (which was calculated as the mean of all oscillations in the ramp after band-pass filtering at 10–120 Hz). That is, as the NCS-1 diffused into the cell, the amplitude and the peak (we will see in Fig. 4 that the mean peak frequency is not affected by this concentration, only the overall power) of the gamma-frequency oscillations increased with time.

Mean oscillation amplitude with 1 μM NCS-1 at the beginning of recording (0 min) was 1.7 $\pm$ 0.2 mV, increased significantly to 6.3 $\pm$ 1.5 mV after 20 min, and remained near this level (df = 6, $F = 4.12$, $P < 0.001$ for ANOVA; post hoc for 20 min $P < 0.002$; post hoc for 25 min $P < 0.04$; post hoc for 30 min $P < 0.03$). Mean oscillation frequency with 1 μM NCS-1 was 37 $\pm$ 3 Hz at *minute 0*, which did not change significantly during the following ramps at 5 min through 30 min (df = 6, $F = 0.30$, P = NS). These findings suggest the modulation of calcium channels presumably located in the dendrites of PPN neurons and promotion of gamma-band oscillation amplitude but not frequency by 1 μM NCS-1. We should note that the amplitude of the oscillations after NCS-1 was at the highest levels we have ever observed, even compared with previously described results using the nonspecific cholinergic agonist carbachol-induced (with and without the stimulant modafinil) oscillations in PPN cells (Kezunovic et al. 2013).

NCS-1 is thought to downregulate N-type calcium channels (Handley et al. 2010). For this reason, we tested the ability of the specific P/Q-type calcium channel blocker to block oscillations potentiated by 1 μM NCS-1. We recorded five cells using electrodes loaded with 1 μM NCS-1 and induced oscillations using ramps, as shown in Fig. 1. We then superfused ω-Aga (200 nM) and found that ramp-induced oscillations that were promoted by NCS-1 were then blocked >70% by ω-Aga (one-way ANOVA, df = 4, $F = 6.43$, $P < 0.001$), suggesting that the oscillations were indeed dependent on P/Q-type calcium channels.

Effects of 10 μM NCS-1 on Gamma-Band Oscillations in PPN Neurons

We then studied the effects of very high concentrations of NCS-1 (10 μM) on beta/gamma-band oscillations in PPN neurons. We determined the effects of NCS-1 at 10 μM passively diffusing intracellularly in PPN neurons during ramp-induced oscillations for up to 30 min. We found that NCS-1 at the 10-μM concentration first increased and then decreased the amplitude of the oscillations in PPN neurons induced by 1-s ramps as it diffused into the cell. Figure 2 is a representative example of ramp-induced membrane potential oscillations in a single PPN neuron in the presence of SB and TTX. Figure 2*A* shows that soon after patching (Fig. 2*A*, black record and black line in the power spectrum in Fig. 2*B*), oscillations were at control amplitude and frequency. After 10 min, the amplitude and frequency of the oscillations were slightly greater in amplitude in this cell (Fig. 2*A*, blue record, and blue line in power spectrum in Fig. 2*B*). However, by 25 min, the amplitude and frequency of oscillations were reduced significantly (Fig. 2*A*, red record, and red line in power spectrum in Fig. 2*B*). Figure 2*C* shows the filtered records from the ramps shown in Fig. 2*A*, demonstrating an initial increase in amplitude at 10 min, followed by a decrease at 25 min. Figure 2*D* shows the power spectrum of the records in Fig. 2*C*, with an initial slight increase in power at min 10 (blue line) compared with *minute 0* (black line) but a marked decrease in power at min 25 (red line). Mean oscillation amplitude with 10 μM NCS-1 at the beginning of recording (0 min) was 2.3 $\pm$ 0.4 mV, which increased significantly at 5 min to 8.2 $\pm$ 1.2 mV (df = 6, $F = 5.76$, $P < 0.01$ for ANOVA; post hoc for 5 min $P < 0.03$) and then gradually decreased until it became

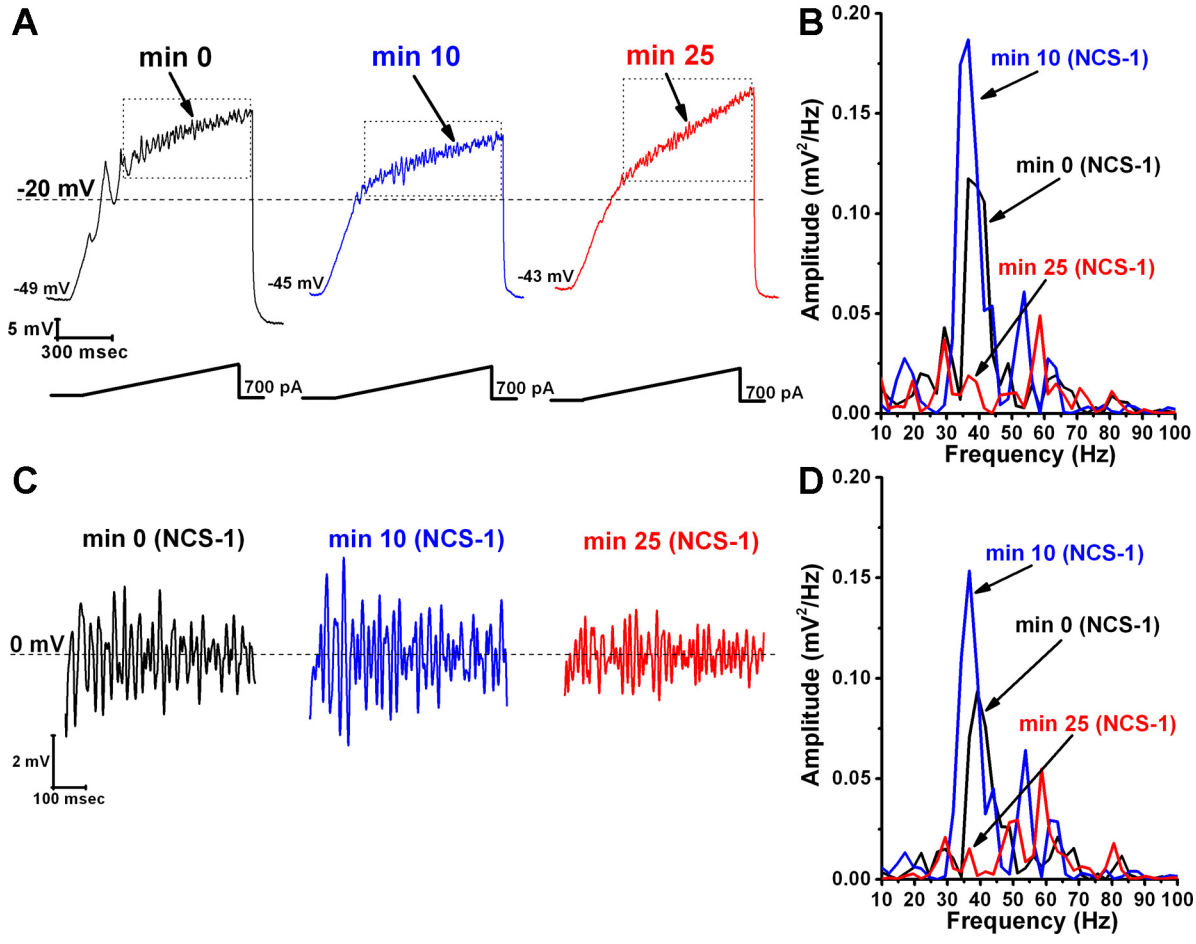

Fig. 2. Effects of NCS-1 at 10 μM on ramp-induced oscillations in PPN neurons. *A*: representative ramp-induced oscillations recorded during 1-s-long current ramps in the presence of SB + TTX and NCS-1 at 10 μM in the recording pipette (*left record*, black). After 10 min of NCS-1 diffusing into the cell, the oscillation amplitude increased slightly (*middle record*, blue). However, testing at 25 min showed a decrease in amplitude compared with both 0- and 10-min recordings (*right record*, red). *B*: power spectrum of the records shown in *A* before band-pass filtering demonstrating the slight increase in amplitude at 10 min and the subsequent decrease at 25 min. *C*: records enclosed by the dotted boxes shown in *A* after band-pass filtering (high pass 10 Hz, low pass 120 Hz). *D*: power spectrum of the records shown in *C* after band-pass filtering. Dashed lines in *A* represent the −20-mV membrane potential, and dashed lines in *C* represent the 0-mV membrane potential.

reduced significantly to 1.2 ± 0.2 mV after 30 min (post hoc for 30 min $P < 0.003$).

Mean oscillation frequency with 10 μM NCS-1 was 43 ± 3 Hz at *minute 0*, which increased significantly at 10 min to 50 ± 3 Hz (df = 6, $F = 2.54$, $P < 0.03$ for ANOVA, post hoc for 10 min $P < 0.05$) but not thereafter. These results suggest that 10 μM NCS-1 can be considered an excessive concentration, beyond physiological levels, which resulted in an initial increase, followed by significant reduction or blockade of gamma-band oscillation amplitude known to be mediated by N- and P/Q-type calcium channels.

Effects of NCS-1 Concentration on PPN Oscillatory Activity

In the present study, we wanted to determine if NCS-1 modulates neuronal activity and how different concentrations affect the frequency and amplitude of calcium channel-mediated oscillations in single PPN neurons. We tested the role of different concentrations of NCS-1 on oscillatory activity by using the same 1-s ramp protocol for all concentrations, along with extracellular solution containing SB + TTX. We tested concentrations of NCS-1 of 0.5, 1, 5, and 10 μM in the recording pipette to allow its diffusion intracellularly only in the recorded neuron. We recorded a group of 25 PPN neurons with different concentrations of NCS-1 and compared their responses to those of 12 PPN cells without NCS-1.

Oscillation frequency, peak power, and mean frequency. Peak power was analyzed by composing a power spectrum and calculating the peak power of the frequency during the entire ramp, basically providing a spectral analysis. Our results show that cells exposed to NCS-1 intracellularly manifested higher frequencies of ramp-induced oscillations at the 5- to 15-min time points but especially at the 20- to 30-min time points. Figure 3 shows that peak power at different frequencies changed over time as NCS-1 diffused into the cell for all four concentrations compared with control cells ("0" concentration). Peak power is represented as the maximum power value per cell in the range of 10–15 Hz (alpha), 15–20 Hz (alpha-beta), 20–30 Hz (beta), and 30–100 Hz (gamma). Statistical analysis showed that 0.5 μM NCS-1 increased peak power significantly in the low frequencies between 10 and 15 Hz at the 5- to 15-min time points (df = 4, $F = 5.1$, $P < 0.001$ for ANOVA; post hoc $P < 0.001$) and also at the 20- to 30-min time points (post hoc $P = 0.01$). We found that 1 μM NCS-1 increased peak power in the 10- to 15-Hz range and the 30- to 100-Hz range at the 20- to 30-time point (post hoc $P < 0.01$). However, 5 μM NCS-1 had no effect on higher frequency ranges (>15 Hz) compared with controls. There was also a significant increase by the 0.5-μM concentration in the 20- to 30-Hz range at 5–15 min (post hoc $P < 0.05$) and at both time points in the 30- to 100-Hz range (post hoc $P < 0.05$). NCS-1 at 1 μM was the only concentration tested that showed a numerical increase in peak power for all frequency ranges (10–100 Hz) after 20 min. At the lowest frequencies analyzed (10–15 Hz), 1 μM NCS-1 significantly increased peak power after 20–30 min (post hoc $P < 0.05$), as well as at the highest frequencies (30–100 Hz) recorded (post hoc $P < 0.05$). Considering only the gamma-frequency range (30–100 Hz), the 0.5- and 1-μM concentrations increased frequency significantly, while the other concentrations (5 and 10 μM) failed to induce significant gamma-band changes.

Mean peak frequency was analyzed as the frequency calculated for the three peak amplitude oscillations in each ramp. Figure 4 shows the mean peak frequencies of ramp-induced oscillations in cells recorded under control conditions (black bars), 0.5 μM (pink bars), 1 μM (blue bars), 5 μM (green bars), and 10 μM (red bars) NCS-1. The only significant change when using 10 μM NCS-1 was a transient increase in mean peak frequency at 10 min (df = 6, $F = 2.54$, $P < 0.03$).

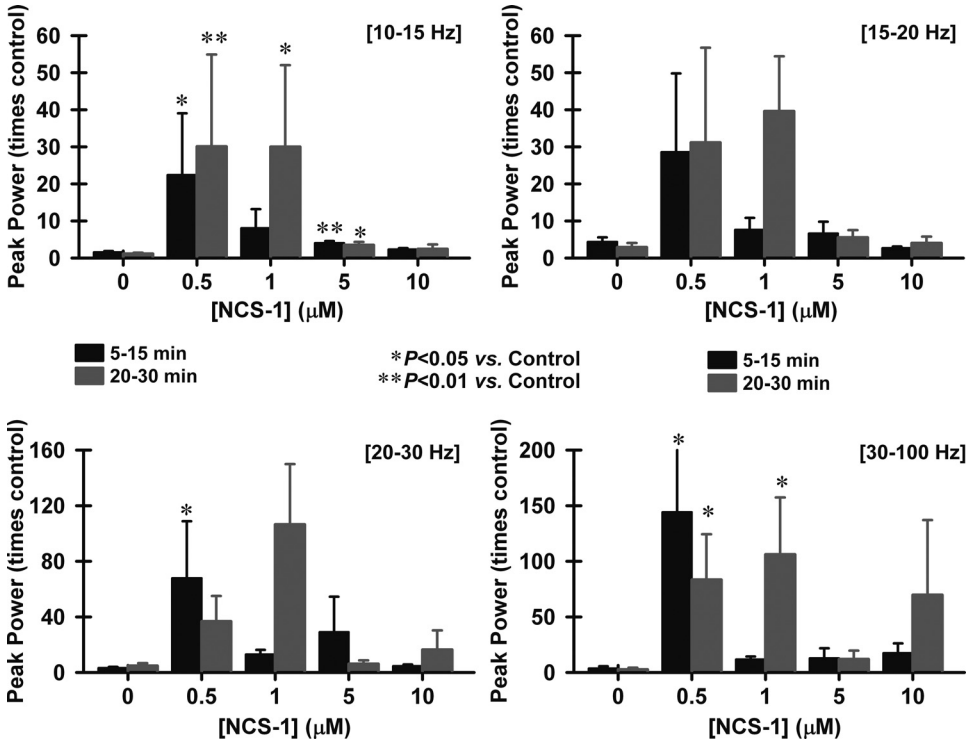

Fig. 3. Effects of NCS-1 on peak power at various frequencies over time. The bar graphs show peak power changing over time at different frequencies as NCS-1 diffused into the cell. Peak power was calculated in the range of 10–15 Hz (alpha, *top left*), 15–20 Hz (alpha-beta, *top right*), 20–30 Hz (beta, *bottom left*), and 30–100 Hz (gamma, *bottom right*). The black bars represent the time point 5–15 min, and the gray bars represent the time points 20–30 min. *$P < 0.05$; **$P < 0.01$. In general, 1 μM NCS-1 significantly increased power at 10–15 Hz and at 30–100 Hz after 20–30 min. There were also variable effects of 0.5 μM NCS-1, with increases at 10–15 Hz at both time points, also at 20–30 Hz, but only after early exposure (5 min), but not later (20–30 min), and at 30–100 Hz but only at 20–30 min.

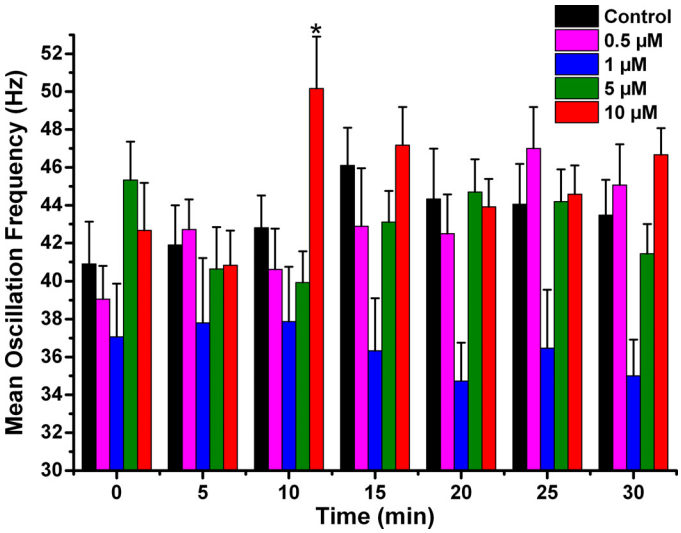

Fig. 4. Effects of NCS-1 on mean peak oscillation frequency over time. The bar graphs show the mean peak frequency calculated from the same three oscillations used to measure peak amplitude. Control cells recorded without NCS-1 shows no significant change over time in mean peak frequency (black bars). Cells recorded using 0.5 μM NCS-1 also showed no significant changes over time (pink bars). Cells recorded using 1 μM NCS-1 did not show changes over time (blue bars), similarly to those recoded using 5 μM NCS-1, which showed no changes (green bars). However, there was an early significant increase in mean peak frequency at 10 min when using 10 μM NCS-1 (red bars). This transient effect did not persist. *$P < 0.05$.

Otherwise, there were no changes in mean peak frequency suggesting that, in general, NCS-1 at most concentrations did not significantly affect mean peak frequency.

Oscillation amplitude. As described above, the control cells (Fig. 5, black bars) showed no significant changes in amplitude throughout the 30-min recording period. These values were not significantly different from each of the 0-min recordings using pipettes with NCS-1, so that the 0-min recordings are an accurate representation of control levels. When the pipette contained 0.5 μM NCS-1 (pink bars), no changes in amplitude were observed throughout the recording, suggesting that this concentration does not significantly affect oscillation amplitude. When 1 μM NCS-1 (blue bars) was used, however, the oscillation amplitude increased significantly by 20 min and thereafter, suggesting a gradual effect in tripling amplitude as the NCS-1 diffused into the cell. When 5 μM NCS-1 (green bars) was used, there was a significant increase in amplitude at 5 min but not afterwards. This transient effect was probably due to the low mean amplitude of the initial oscillations in this group of cells compared with the mean amplitude they exhibited between 5 and 30 min. Moreover, comparing the variance in the cells tested using 5 μM NCS-1, at the initial 0-min time point, these showed a very low variance, thus allowing the tests used to find positive statistical differences in the presence of relatively small changes induced by such concentration of NCS-1. There were no further changes observed, so that we conclude that the effect at 5 min was not consistent. When using 10 μM NCS-1 (red bars), the oscillation amplitude immediately increased to four times the levels at 5 min and gradually decreased until it was significantly reduced by 30 min. These effects suggest an immediate effect on amplitude by very high levels of NCS-1 that ultimately led to partial blockade. Based on these results, 1 μM NCS-1 seems to be the most critical concentration for gamma oscillation modulation, although the transient effect mentioned above was evident with 5 μM NCS-1.

Calcium Currents

To evaluate the effects of NCS-1 on high-threshold, voltage-dependent calcium currents (I_{Ca}) present in PPN neurons (n = 27), square voltage steps were used in combination with high-cesium/QX314 intracellular pipette solution and synaptic receptor blockers (see METHODS). High-threshold current I–V curves and time course did not change across PPN cell types (data not shown). Calcium currents were recorded after gaining access to the neuronal intracellular compartment and the series resistance was compensated and stable. Recordings of the calcium currents lasted for up to 30 min without significant rundown, as previously reported (Kezunovic et al. 2011, 2013). The holding potential was initially clamped at −50 mV and then depolarized up to 0 mV. These square voltage steps were applied shortly after breaking into the cell and applied every 5 min for up to 30 min. Figure 6 shows the results of the calcium current study carried out using NCS-1 concentrations of 0.5, 1, and 10 μM NCS-1. Figure 6*A* shows the voltage step protocol and representative calcium currents at *minute 0* through *minute 15* using NCS-1 at 1 μM. Subsequent time points were similar to 15 min and are not shown. Figure 6*B* shows the time course of mean reduction of I_{Ca} by 0.5 μM (black circles), 1 μM (light gray circles), and 10 μM NCS-1 (dark gray squares). All curves were well fitted to a single exponential ($R^2 > 0.99$, dotted lines), yielding tau (τ) values of and 9.4, 7.8, and 8.8 min for 0.5-μM, 1-μM NCS-1, and 10-μM curves, respectively. Two-way ANOVA statistical comparison showed no interaction between [NCS-1] × time (min) [$F_{(6,75)} = 0.6$; $P >$

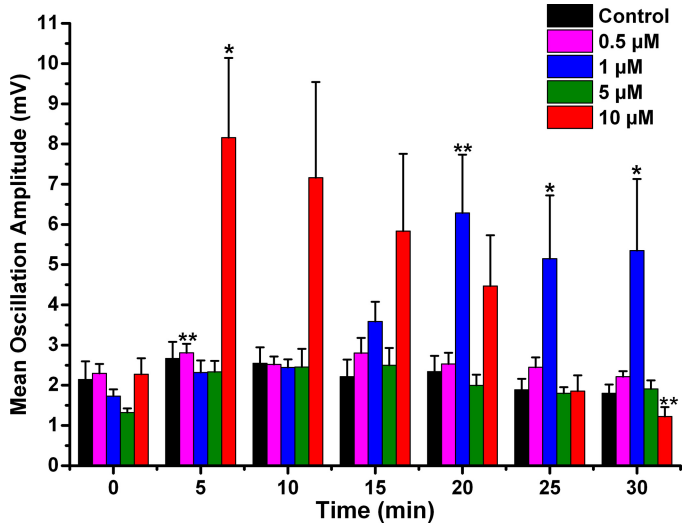

Fig. 5. Effects of NCS-1 on mean peak oscillation amplitude over time. The bar graphs show the mean peak amplitude in mV of oscillations calculated by measuring the 3 highest amplitude oscillations after filtering to derive mean amplitude. Control cells recorded (black bars) demonstrate no significant changes over time. Cells recorded using 0.5 μM NCS-1 also showed no significant changes over time (pink bars). Cells recorded using 1 μM NCS-1 (blue bars) showed significant increases in mean peak oscillation amplitude at 20 min through 30 min. Cells recoded using 5 μM NCS-1 (green bars) showed no significant changes over time, but cells recorded using 10 μM NCS-1 (red bars) showed a significant increase in mean peak oscillation amplitude at 5 min and a significant decrease at 30 min. *$P < 0.05$; **$P < 0.01$.

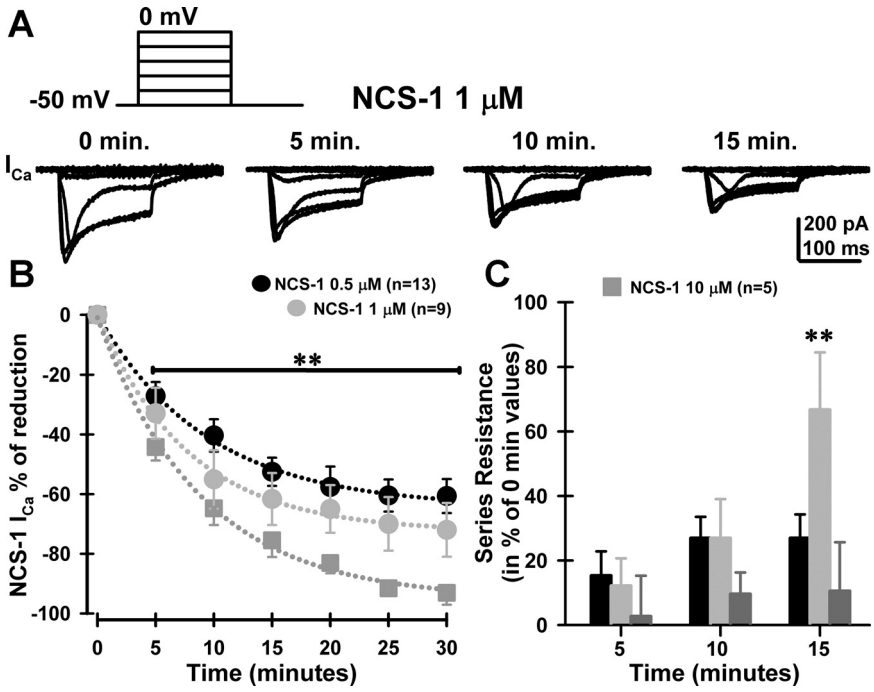

Fig. 6. Effects of NCS-1 on voltage-dependent calcium currents (I_{Ca}) in PPN cells. *A*: representative I_{Ca} recorded using 5 depolarizing square steps from −40 to 0 mV from −50-mV holding potential over time (0, 5, 10, and 15 min of exposure) using 1 μM NCS-1. *B*: mean time course of I_{Ca} block by intracellular 0.5 μM (black circles; $n = 13$ PPN neurons), 1 μM (light gray circles; $n = 9$ PPN neurons), and 10 μM (dark gray squares; $n = 5$ PPN neurons). Data points were fitted to a single exponential decay yielding tau (τ) values of 9.4, 7.8, or 8.8 min for 0.5-, 1-, or 10-μM NCS-1 curves, respectively. $^{**}P < 0.001$, Kruskal-Wallis one-way ANOVA, df = 2, $H > 102$, comparing 10-μM to 0.5-μM and 1-μM %block after 5 min of NCS-1 exposure. *C*: series resistance change (in % of 0-min values) observed at 5, 10, and 15 min after exposure to either 0.5 μM NCS-1 (black bars), 1 μM NCS-1 (light gray bars), or 10 μM (dark gray bars) NCS-1. Series resistance values reached a plateau after 15 min, when using 1 μM NCS-1. $^{**}P < 0.001$, one-way ANOVA, $F_{(2,25)} = 60$; post hoc Bonferroni *t*-test, 1 vs. 10 μM, $t = 9$, $P < 0.001$; 1 vs. 0.5 μM, $t = 9.9$, $P < 0.001$; 1 vs. 0.5 μM, $t = 1.3$, $P > 0.05$.

0.05]. Significant differences were observed over time [$F_{(6,75)} = 131$; $P < 0.001$], while a Kruskal-Wallis one-way ANOVA (df = 2, $H > 102$), comparing 10-μM to the 0.5-μM and 1-μM %block after 5 min of NCS-1 exposure was significantly different ($P < 0.001$). Although the effects of all concentrations on calcium currents were significant, the time course of the effects was similar and concentration dependent. This suggests that the exponential fitting indicates that intracellular pathways are being affected with a similar time course. Current studies are investigating the various intracellular pathways by which NCS-1 is acting in PPN neurons.

Furthermore, an increase in series resistance was observed after 15 min during the 1-μM NCS-1 experiments [Fig. 6*C*, one-way ANOVA, $F_{(2,25)} = 60$; post hoc Bonferroni *t*-test, 1 vs. 10 μM, $t = 9$, $P < 0.001$; 1 vs. 0.5 μM, $t = 9.9$, $P < 0.001$; 1 vs. 0.5 μM, $t = 1.3$, $P > 0.05$]. Series resistance values reached a plateau after 15 min, when using 1 μM NCS-1 but not when using the lower or higher concentrations.

DISCUSSION

We previously showed that, regardless of cell type, voltage-dependent, high-threshold P/Q-type calcium channel activation mediates beta/gamma-frequency oscillatory activity in all PPN neurons (Kezunovic et al. 2011). The findings obtained demonstrate that intracellular NCS-1 can exert a concentration-dependent biphasic effect on gamma-band oscillatory activity of PPN neurons. While lower NCS-1 concentrations such as 1 μM enhanced oscillation frequency and amplitude only after 20 min, 10 μM had a very early (within 5–15 min) enhancing effect of oscillation amplitude, followed by an inhibitory effect, ultimately reducing the amplitude and frequency of gamma oscillations by 30 min. Moreover, low intracellular NCS-1 concentrations (both 0.5 and 1 μM) were able to reduce the amplitude of PPN calcium currents within 5 to 15 min. Strikingly, the time course of the calcium current block (~5–15 min, Fig. 6) was similar to the 10-μM NCS-1 effect on oscillation amplitude (~5–15 min, Fig. 5), but both of these effects were faster than the one observed for the enhancement of gamma-band amplitude and gamma frequency of oscillations (>20 min, Fig. 5), suggesting that multiple intracellular mechanisms may mediate the NCS-1 effects on PPN oscillations.

For example, NCS-1 appears to facilitate P/Q-type calcium channel currents (Tsujimoto et al. 2002) and also regulate inositol triphosphate receptor (InsP3) activity (Kasri et al. 2004). The InsP3 receptor is present in the PPN (Rodrigo et al. 1993). We assume that activation of muscarinic cholinergic receptors will trigger a G protein-coupled pathway (Kezunovic et al. 2013) that releases InsP3, which acts with cytoplasmic NCS-1 to bind to the InsP3 receptor in the endoplasmic reticulum to release intracellular calcium. Consequently, it is that release that potentiates calcium channel mediated currents. Much research is required to substantiate these suggestions.

Concentration of NCS-1 and Intracellular Ca^{2+} Concentration Dynamics

Previous in vitro experiments determined that NCS-1 activated two calmodulin-dependent enzymes (Schaad et al. 1996). These authors found that 1 μM NCS-1 was maximally effective, while higher concentrations were less potent in activating these enzymes. This study also found that 1 μM NCS-1 potentiated nitric oxide synthase two to four times, which was an effect that saturated at 10 μM NCS-1. They concluded that NCS-1 represents an ideal switch for neurons to respond rapidly to slight variations in internal calcium concentrations. We elected to test 1 and 10 μM NCS-1 for our initial studies as a result of these findings. Based on the human post mortem results showing overexpression of NCS-1 in the brains of schizophrenic and bipolar disorder patients, but not in normal controls or major depression patients (Koh et al. 2003), we hypothesized the following. While the mean increase in NCS-1 was in the order of 50%, the individual levels between the

lowest level in a control subject and the highest level in a schizophrenic or bipolar disorder patient was in the order of five- to eightfold (see Fig. 2 in Koh et al. 2003). Therefore, we expected that, if 1 μM was an optimal concentration for the normal effect of NCS-1, then a 10-fold increase, or 10 μM NCS-1, would be an excessive level in keeping with significant overexpression. Our results indeed showed that NCS-1 at 1 μM promoted gamma-band oscillations in PPN neurons (tripled amplitude, increased power at all frequencies), while NCS-1 at 10 μM at first potentiated (quadrupled amplitude, no effect on frequencies) but soon significantly reduced, the oscillations. We assume that the low levels of NCS-1 slowly activate greater and greater numbers of channels as the concentration increases, peaking after 20 min using 1 μM NCS-1. However, when exposed to 10 μM NCS-1, the large amounts initially activate channels within 5–15 min, but then saturate the process, slowly leading to shutting down of the effect, so that by 30 min there is a net decrease in oscillation amplitude. This saturation process is probably due to an intracellular mechanism as yet identified. To some degree, the results on frequency (Fig. 3) and amplitude (Fig. 4) also suggest that there is an early effect that is different from the later effect, as we observed in the calcium current results. As far as gamma-band frequencies are concerned, only 0.5 and 1 μM NCS-1 increased power, while higher concentrations (5 and 10 μM) failed to increase gamma-band power (Fig. 3). The fact that oscillation frequency does not change suggests that the kinetics of the calcium channels is not changing, but the increase in amplitude implies that the flow of calcium through the calcium channels is increasing, possibly because more channels are opening.

The increase in series resistance suggests that at least some channels are closing after 15 min of exposure. Since we used high-Cs^+ intracellularly and extracellular TEA, plus SB and TTX, all potassium and sodium channels were blocked, so that the increase in input resistance is likely from closing some calcium channels. This particular intracellular effect is also being currently investigated, but the most likely explanation is that NCS-1 is known to downregulate N-type calcium channels (Handley et al. 2010). The increase in input resistance seen after 15 min using 1 μM NCS-1 may be due to the inactivation of these channels. When 10 μM NCS-1 were used, this effect may have occurred too rapidly to detect due to the large concentration of NCS-1.

Calcium participates in a myriad of neuronal processes, and its metabolism is tightly controlled. For example, neurite outgrowth does not occur if there is too little calcium and growth stops if there is too much, suggesting that a narrow window is essential for neurite outgrowth (Kater and Mills, 1991). NCS-1 is known to modulate the optimal level of calcium necessary for neurite outgrowth (Hui et al. 2007). Therefore, we speculate that NCS-1 at optimal concentrations will help maintain gamma-band oscillations dependent on P/Q-type calcium channels but too little or too much will lead to a decrease or interrupted pattern of gamma-band activity. The use of ω-Aga blocked ramp-induced oscillations when using 1 μM NCS-1, suggesting that indeed P/Q-type calcium channels are responsible for these oscillations. Our previous studies found that P/Q-type calcium channels were essential for gamma oscillations in the PPN, while N-type channels were permissive (Kezunovic et al. 2011). Since NCS-1 is known to downregulate N-type calcium channels (Handley et al. 2010), we assume that these are the channels being blocked when input resistance increased (Fig. 5).

The biphasic effects on intracellular Ca^{2+} concentration ($[Ca^{2+}]$) have been previously described to affect the time course of calcium channel inactivation (Cox and Dunlap 1994). In addition, two separate $[Ca^{2+}]$ transients (both from intracellular stores and present throughout membrane calcium channels) were observed when muscarinic, but not nicotinic, receptors were activated (Forsythe et al. 1992). A significant increase in the formation of intracellular inositol phosphate occurred during intracellular $[Ca^{2+}]$ transients. In cortical neurons, glutamate-dependent membrane depolarization affected intracellular $[Ca^{2+}]$ in a biphasic manner, which was found to modulate extracellular signal-regulated kinase 1/2 (ERK1/2) signaling as well as cAMP-responsive element binding protein (CREB) phosphorylation, and increased gene expression of brain-derived neurotrophic factor (BDNF) (Dravid et al. 2004). Furthermore, Na^+ and Ca^{2+} influx triggered by membrane depolarization has been described to mediate a biphasic stimulatory effect followed by an inhibitory regulation of adenylyl cyclase in cerebellar granule cells (Cooper et al. 1998). The biphasic effects described here could be mediated by a rapid recruitment of calcium channels and its known downstream intracellular modulatory machinery (e.g., intracellular G-protein modulation; Kezunovic et al. 2013) by NCS-1 at 1 μM, while a more extreme $[Ca^{2+}]$-buffering by NCS-1 at 5–10 μM could interfere with downstream elements. Future experiments are needed to further confirm this hypothesis.

We assume that the reason why 1 μM NCS-1 increased oscillation amplitude was because an intracellular pathway was recruited that helps maintain oscillations for prolonged periods, perhaps through the mechanisms described above. The increase observed with 10 μM may indicate a response to a bolus of NCS-1 that soon (with 5–15 min) saturated the substrate available for its action and ultimately led to a decrease in oscillation amplitude (>30 min). The effects of 5 μM NCS-1 would be expected to cause changes both early and late, but do not, suggesting that this concentration rapidly saturates two different intracellular mechanisms. Below, we discuss the possibility that overexpression of NCS-1 in the brains of schizophrenic and bipolar disorder patients may be approximately five times normal, which could account for the decrease in gamma-band oscillations observed in these disorders.

Clinical Implications

Schizophrenia is characterized by abnormalities in wake-sleep control, including hypervigilance; decreased slow wave sleep, especially deep sleep stages; increased REM sleep drive; and fragmented sleep (Caldwell and Domino 1967; Feinberg et al. 1969; Itil et al. 1972; Jus et al. 1973; Zarcone et al. 1975). These wake-sleep abnormalities reflect increased vigilance and REM sleep drive, i.e., overactive RAS output. The increased REM sleep drive has been proposed to account for REM sleep intrusion during waking, that is, in eliciting hallucinations (Dement 1967; Mamelak and Hobson 1989). We assume that the changes observed following exposure to NCS-1 in PPN cells have direct relevance to these seriously disturbed wake-sleep symptoms.

The results presented suggest that NCS-1 concentrations of ~1 μM lead to long-lasting increases in gamma-band oscillation amplitude and frequency. Higher concentrations such as 5 μM appear to block these effects, while excessive concentrations like 10 μM trigger very high-amplitude oscillations that then slowly decrease until they are of below normal amplitude. These effects point to high concentrations of NCS-1 as down-regulating gamma-band activity duration and amplitude. Decreases in gamma-band coherence and maintenance can account for many of the symptoms of schizophrenia and perhaps bipolar disorder. The positive symptoms include hallucinations, delusions, thought disorder, and agitation, while negative symptoms include lack of affect, anhedonia, and withdrawal. Cognitive symptoms include poor executive function, lack of attention, and disturbed working memory. All of these cognitive functions are associated with gamma-band activity. The postmortem results previously described (Koh et al. 2003) suggest that only some patients with schizophrenia may suffer from significant overexpression of NCS-1, which may be manifested as decreased gamma-band activity only in a subpopulation of patients. No human study has measured gamma-band activity and correlated it with NCS-1 levels. Unfortunately, serum sampling does not reflect brain levels and, in fact, NCS-1 levels in leukocytes are actually decreased in schizophrenic patients (Torres et al. 2009). However, future clinical trials in patients with schizophrenia or bipolar disorder may benefit from prior determination of a significant decrease in gamma-band activity, which may also help address the heterogeneity of schizophrenia and facilitate the process of identifying more homogeneous groups within the syndrome (Picardi et al. 2012). It is to those patients that pharmacological targeting to increase gamma-band activity may be of benefit. These effects may not apply to those patients that exhibit increased gamma-band activity (Andreou et al. 2014; Diez et al. 2014), further emphasizing the heterogeneous nature of the population. We have preliminary evidence suggesting that the stimulant modafinil may indeed compensate to some extent for excessive amounts of NCS-1. We found a partial return of gamma oscillations that were suppressed by high levels (10 μM) of NCS-1 after exposure to modafinil (Garcia-Rill et al. 2014). However, additional research is essential to determine the potential use of this agent in patients selected specifically for decreased gamma-band activity.

In keeping with the roles of this nucleus, we assume that overexpression of NCS-1 in PPN neurons in some patients can account for the decreased and interrupted gamma-band activity related to arousal and REM sleep. Since NCS-1 is probably overexpressed throughout the brain, we conclude that gamma-band activity dependent on calcium channels would be disrupted in all regions that use this mechanism, for example, in the cortex, thalamus, cerebellum, and hippocampus.

GRANTS

This work was supported by National Institutes of Health (NIH) Grant R01-NS-020246 and by core facilities of the Center for Translational Neuroscience supported by NIH Grants P20-GM-103425 and P30-GM-110702 (to E. Garcia-Rill). In addition, this work was supported by FONCYT-Agencia Nacional de Promoción Científica y Tecnológica Grants BID 1728 OC.AR. PICT 2008-2019 and PICT-2012-1769 (to F. J. Urbano).

DISCLOSURES

No conflicts of interest, financial or otherwise, are declared by the author(s).

AUTHOR CONTRIBUTIONS

Author contributions: S.M.D., N.K., J.R.H., and B.L. performed experiments; S.M.D., N.K., B.L., F.J.U., and E.G.-R. analyzed data; S.M.D., N.K., E.M., and E.G.-R. interpreted results of experiments; S.M.D., N.K., J.R.H., B.L., and F.J.U. prepared figures; S.M.D., E.M., F.J.U., and E.G.-R. edited and revised manuscript; S.M.D., N.K., J.R.H., B.L., E.M., F.J.U., and E.G.-R. approved final version of manuscript; E.M., F.J.U., and E.G.-R. conception and design of research; E.G.-R. drafted manuscript.

REFERENCES

Andreou C, Nolte G, Leicht G, Polomac N, Hanganu-Opatz IL, Lambert M, Mulert C. Incresaed resting-state gamma-band connectivity in first-episode schizophrenia. *Schizophr Bull* 2014 Aug 28 [Epub ahead of print].

Bergson C, Levenson R, Goldman-Rakic P, Lidow MS. Dopamine receptor-interacting proteins: the Ca^{2+} connection in dopamine signaling. *Trends Pharmacol Sci* 24: 486–492, 2003.

Brucke C, Huebl J, Schonecker T, Wof-Julian N, Yarrow K, Kupsch A, Blahak C, Lutjens G, Brown P, Krauss J, Schneider GH, Kuhn A. Scaling of movement is related to pallidal γ oscillations in patients with dystonia. *J Neurosci* 32: 1008–1019, 2012.

Buzsáki G. *Rhythms of the Brain*. Oxford, UK: Oxford Univ. Press, 2006, p. 253–254.

Caldwell DF, Domino EF. Electroencephalographic and eye movement patterns during sleep in chronic schizophrenic patients. *Elecetroenceph Clin Neurophysiol* 22: 414–420, 1967.

Charpak S, Paré D, Llinás RR. The entorhinal cortex entrains fast CA1 hippocampal oscillations in the anaesthetized guinea-pig: role of the monosynaptic component of the perforant path. *Eur J Neurosci* 7: 1548–1557, 1995.

Cheyne G, Ferrari P. MEG studies of motor cortex gamma oscillations: evidence for a gamma "fingerprint" in the brain? *Front Hum Neurosci* 7: 575, 2013.

Chrobak JJ, Buzsáki G. Gamma oscillations in the entorhinal cortex of the freely behaving rat. *J Neurosci* 18: 388–398, 1998.

Cooper DM, Schell MJ, Thorn P, Irvine RF. Regulation of adenylyl cyclase by membrane potential. *J Biol Chem* 273: 27703–27707, 1998.

Cox DH, Dunlap K. Inactivation of N-type calcium current in chick sensory neurons: calcium and voltage dependence. *J Gen Physiol* 104: 311–336, 1994.

Dement WC. Studies on the effects of REM deprivation in humans and animals. *Res Publ Assoc Res Nerv Ment Dis* 43: 456–467, 1967.

Diez A, Suazo V, Casado P, Martin-Loeches M, Molina V. Gamma power and cognition in patients with schizophrenia and their first-degree relatives. *Neuropsychobiology* 69: 120–128, 2014.

D'Onofrio S, Kezunovic N, Urbano FJ, Garcia-Rill E. *Novel Treatment for Schizophrenia* (Abstract). Washington DC: IDeA Meeting, 2014.

Dravid SM, Baden DG, Murray TF. Brevetoxin activation of voltage-gated sodium channels regulates Ca dynamics and ERK1/2 phosphorylation in murine neocortical neurons. *J Neurochem* 89: 739–749, 2004.

Eckhorn R, Bauer R, Jordan W, Brosch M, Kruse W, Munk M, Reitboeck HJ. Coherent oscillations: a mechanism of feature linking in the visual system? Multiple electrode and correlation analyses in the cat. *Biol Cybern* 60: 121–130, 1988.

Feinberg I, Braun M, Koresko RL, Gottleib F. Stage 4 sleep in schizophrenia. *Arch Gen Psychiatry* 21: 262–266, 1969.

Forsythe ID, Lambert DG, Nahorski SR, Lindsdell P. Elevation of cytosolic calcium by cholinoceptor agonists in SH-SY5Y human neuroblastoma cells: estimation of the contribution of voltage-dependent currents. *Br J Pharmacol* 107: 207–214, 1992.

Garcia-Rill E, Heister DS, Ye M, Charlesworth A, Hayar A. Electrical coupling: novel mechanism for sleep-wake control. *Sleep* 30: 1405–1414, 2007.

Garcia-Rill E, Charlesworth A, Heister DS, Ye M, Hayar A. The developmental decrease in REM sleep: the role of transmitters and electrical coupling. *Sleep* 31: 673–690, 2008.

Garcia-Rill E. Sleep and arousal states: reticular activating system. In: *New Encyclopedia of Neuroscience*, edited by Squire LR, Bloom F, Spitzer N, Gage F, Albright T. Oxford, UK: Elsevier, 2009, vol. 8, p.137–143.

Garcia-Rill E, Kezunovic N, Hyde J, Beck P, Urbano FJ. Coherence and frequency in the reticular activating system (RAS). *Sleep Med Rev* 17: 227–238, 2013.

Garcia-Rill E, Kezunovic N, D'Onofrio S, Luster B, Hyde J, Bisagno V, Urbano FJ. Gamma band activity in the RAS-intracellular mechanisms. *Exp Brain Res* 232: 1509–1522, 2014.

Gray CM, Singer W. Stimulus-specific neuronal oscillations in orientation columns of cat visual cortex. *Proc Natl Acad Sci USA* 86: 1698–1702, 1989.

Handley MT, Lian LY, Haynes LP, Burgoyne RD. Structural and functional deficits in a neuronal calcium sensor-1 mutant identified in a case of autistic spectrum disorder. *PLoS One* 5: E10534, 2010.

Hui K, Fei GH, Saab BJ, Su J, Roder JC, Feng ZP. Neuronal calcium sensor-1 modulation of optimal calcium for neurite outgrowth. *Development* 134: 4479–4489, 2007.

Hyde J, Kezunovic N, Urbano FJ, Garcia-Rill E. Visualization of fast calcium oscillations in the parafascicular nucleus. *Pflügers Arch* 465: 1327–1340, 2013a.

Hyde J, Kezunovic N, Urbano FJ, Garcia-Rill E. Spatiotemporal properties of high speed calcium oscillations in the pedunculopontine nucleus. *J Appl Physiol* 115: 1402–1414, 2013b.

Itil TM, Hsu W, Klingenberg W, Saletu B, Gannon P. Digital computer-analyzed all-night sleep EEG patterns (sleep prints) in schizophrenics. *Biol Psychiatry* 4: 3–16, 1972.

James W. *The Principles of Psychology* (originally published in 1890). New York: Cosimo Classics, 2007, p. 84.

Jenkinson N, Kuhn AA, Brown P. Gamma oscillations in the human basal ganglia. *Exp Neurol* 245: 72–76, 2013.

Jouvet-Mounier D, Astic L, Lacote D. Ontogenesis of the states of sleep in rat, cat, and guinea pig during the first postnatal month. *Dev Psychobiol* 2: 216–39, 1970.

Jus K, Bouchard M, Jus A, Villeneuve A, Lachance R. Sleep EEG studies in untreated long-term schizophrenic patients. *Arch Gen Psychiatry* 29: 286–290, 1973.

Kasri NN, Holmes AM, Bultynk G, Parys JB, Bootman MD, Rietdorf K, Missiaen L, McDonald F, Smedt H, Conway SJ, Holmes AB, Berridge MJ, Roderick HL. Regulation of $InsP_3$ receptor activity by neuronal Ca^{2+}-binding proteins. *EMBO J* 23: 312–321, 2004.

Kater SB, Mills LR. Regulation of growth cone behavior by calcium. *J Neurosci* 11: 891–899, 1991.

Kezunovic N, Urbano FJ, Simon C, Hyde J, Garcia-Rill E. Mechanism behind gamma band activity in the pedunculopontine nucleus. *Eur J Neurosci* 34: 404–415, 2011.

Kezunovic N, Hyde J, Simon C, Urbano FJ, Williams DK, Garcia-Rill E. Gamma band activity in the developing parafascicular nucleus. *J Neurophysiol* 107: 772–784, 2012.

Kezunovic N, Hyde J, Goitia B, Bisagno V, Urbano FJ, Garcia-Rill E. Muscarinic modulation of high frequency activity in pedunculopontine neurons. *Front Neurol* 4: 176, 2013.

Koh PO, Undie AS, Kabbani N, Levenson R, Goldman-Rakic P, Lidow MS. Up-regulation of neuronal calcium sensor-1 (NCS-1) in the prefrontal cortex of schizophrenic and bipolar patients. *Proc Natl Acad Sci USA* 100: 313–317, 2003.

Lalo E, Thobois S, Sharott A, Polo G, Mertens P, Pogosyan A. Patterns of bidirectional communication between cortex and basal ganglia during movement in patients with Parkinson disease. *J Neurosci* 28: 3008–3016, 2008.

Lang EJ, Sugihara I, Llinás RR. Olivocerebellar modulation of motor cortex ability to generate vibrissal movements in rat. *J Physiol* 571: 101–120, 2006.

Litvak V, Eusebio A, Jha A, Oosterveld R, Barnes G, Foltynie T. Movement-related changes in local and long-range synchronization in Parkinson's disease revealed by simultaneous magnetoencephalography and intracranial recordings. *J Neurosci* 32: 10541–10553, 2012.

Mamelak AN, Hobson JA. Dream bizarreness as the cognitive correlate of altered neuronal brain in REM sleep. *J Cogn Neurosci* 1: 201–222, 1989.

Pedroarena C, Llinas RR. Interactions of synaptic and intrinsic electroresponsiveness determine corticothalamic activation dynamics. *Thalam Rel Syst* 1: 3–14, 2001.

Picardi A, Viroli C, Tarsitani L, Miglio R, de Girolamo G, Dell'Acqua G, Biondi M. Heterogeneity and symptom structure of schizophrenia. *Psychiatry Res* 198: 386–394, 2012.

Philips S, Takeda Y. Greater frontal-parietal synchrony at low gamma-band frequencies for inefficient than efficient visual search in human EEG. *Int J Psychophysiol* 73: 350–354, 2009.

Ozerdem A, Guntenkin B, Atagun I, Turp B, Basar E. Reduced long distance gamma (28–48 Hz) coherence in euthymic patients with bipolar disorder. *J Affect Disord* 132: 325–332, 2011.

Rodrigo J, Suburu AM, Bentura ML, Fernandez T, Nakada S, Mikoshiba K, Martinez-Murillo R, Polak JM. Distribution of the inositol 1,4,5-triphosphate receptor, P400, in adult rat brain. *J Comp Neurol* 337: 493–517, 1993.

Schaad NC, De Castro E, Nef S, Hegi S, Hinrichsen R, Martone ME, Ellisman MH, Sikkink R, Rusnak F, Sygush J, Nef P. Direct modulation of calmodulin targets by the neuronal calcium sensor NCS-1. *Proc Natl Acad Sci USA* 93: 9253–9258, 1996.

Simon C, Kezunovic N, Ye M, Hyde J, Hayar A, Williams DK, Garcia-Rill E. Gamma band unit activity and population responses in the pedunculopontine nucleus. *J Neurophysiol* 104: 463–474, 2010.

Singer W. Synchronization of cortical activity and its putative role in information processing and learning. *Annu Rev Physiol* 55: 349–374, 1993.

Soteropoulos DS, Baker SN. Cortico-cerebellar coherence during a precision grip task in the monkey. *J Neurophysiol* 95: 1194–1206, 2006.

Spencer KM, Nestor PG, Niznikiewicz MA, Salisbury DF, Shenton ME, McCarley RW. Abnormal neural synchrony in schizophrenia. *J Neurosci* 23: 7407–7411, 2003.

Timofeev I, Steriade M. Fast (mainly 30–100 Hz) oscillations in the cat cerebellothalamic pathway and their synchronization with cortical potentials. *J Physiol* 504: 153–168, 1997.

Torres KC, Souza BR, Miranda DM, Sampiao AM, Nicolato R, Neves FS, Barros AG, Dutra WO, Gollob KJ, Correa H, Romano-Silva MA. Expression of neuronal calcium sensor-1 (NCS-1) is decreased in leukocytes of schizophrenia and bipolar disorder patients. *Prog Neuropsychopharmacol Biol Psychiatry* 33: 229–234, 2009.

Trottenberg T, Fogelson N, Kuhn AA, Kivi A, Kupsch A, Schneider GH, Brown P. Subthalamic gamma activity in patients with Parkinson's disease. *Exp Neurol* 200: 56–65, 2006.

Tsujimoto T, Jeromin A, Saitoh N, Roder JC, Takahashi T. Neuronal calcium sensor 1 and activity-dependent facilitation of P/Q-type calcium currents at presynaptic nerve terminals. *Science* 295: 2276–2279, 2002.

Uhlhaas PJ, Singer W. Abnormal neural oscillations and synchrony in schizophrenia. *Nat Rev Neurosci* 11: 100–113, 2010.

Urbano FJ, Kezunovic N, Hyde J, Simon C, Beck P, Garcia-Rill E. Gamma band activity in the reticular activating system. *Front Neurol* 3: 1–16, 2012.

Wang HL, Morales M. Pedunculopontine and laterodorsal tegmental nuclei contain distinct populations of cholinergic, glutamatergic and GABAergic neurons in the rat. *Eur J Neurosci* 29: 340–358, 2009.

Ye M, Hayar A, Strotman B, Garcia-Rill E. Cholinergic modulation of fast inhibitory and excitatory transmission to pedunculopontine thalamic projecting neurons. *J Neurophysiol* 103: 2417–2432, 2010.

Zarcone V, Azumi K, Dement W, Gulevich G, Kraimer H, Pivik R. REM phase deprivation and schizophrenia II. *Arch Gen Psychiatry* 32: 1431–1436, 1975.